ISBN: 978-3-95450-234-9 ISSN: 2673-5504 doi:10.18429/JACoW-SRF2023-WEPWB085

DEGRADATION AND RECOVERY OF CAVITY PERFORMANCE IN SRILAC CRYOMODULES AT RIBF

N. Sakamoto*, O. Kamigaito, K. Ozeki, K. Suda, K. Yamada
RIKEN Nishina Center, Saitama, Japan

Abstract

The RIKEN superconducting (SC) heavy-ion linear accelerator (SRILAC) has been providing beam supply for super-heavy elements synthesis experiments [1] since its commissioning in January 2020 [2]. However, the long-term operation of SC radio-frequency (RF) cavities leads an increase in the X-ray levels caused by field emissions resulting from changes in the inner surface conditions. More than half of the ten SC 1/4 wavelength resonators (SC-QWRs) of SRILAC, operating at a frequency of 73 MHz, have experienced an increase in X-ray levels, thus, requiring adjustments to the acceleration voltage for continuous operation. While several conditioning methods have been employed for SC cavities, a fully established technique is yet to be determined. To address this situation, a relatively simple conditioning method was implemented at RIKEN. The proposed method uses high-voltage pulsed power and imposes a low load on the cavities.

INTRODUCTION

The mission of the RIKEN Radioactive Isotope Beam Factory (RIBF) [3] is to improve our understanding of the mechanism underlying the synthesis of elements by performing experiments using intense heavy-ion beams. At the RIBF, heavy-ion beams at various energies are available, from sub-coulomb energy levels employed for fusion reactions to intermediate energy levels for radioisotope beam production using fission reactions. Beams of ion species ranging from H to U are accelerated in accordance with experimental requirements. The RIBF accelerator complex consists of booster ring cyclotrons and three injectors, namely the azimuthally varying field (AVF) cyclotron, the RIKEN liner accelerator (RILAC), and a second linear accelerator (RILAC2), as shown in Fig. 1. The velocity change of heavy ions is moderate during acceleration. Therefore, various accelerator structures are combined. The frequency tunable accelerators of RIBF enable the usage of various ion species with different energies. To achieve an increasingly high beam power, several efforts have been made in terms of improving performance and reliability of each component of the accelerators. One of the injector linacs, RILAC, was upgraded to enable a new element synthesis experiment at the RIKEN RIBF.

In 2016, a new comprehensive superheavy element (SHE) research program commenced at the RIKEN Nishina Center (RNC). The main objective was to expand the periodic table of elements by synthesizing new superheavy elements. After the synthesis of oganesson (Z = 118), the aim of the SHE project was to synthesize an element with Z > 118. Aiming to synthesize the element with Z = 119, at the RNC we adopted a ^{51}V as the beam and ^{248}Cm as the target. For this experiment, the required beam energy was higher than 6 MeV/u with an intensity of 2.5 pμA. Thus, the primary aim of this project was to upgrade of the accelerator by introducing a SC linear accelerator to increase the final beam energy from 5.5 to 6.5 MeV/u, and a SC electron-cyclotron-resonance ion source (ECRIS) to multiply the beam intensity by a factor of five.

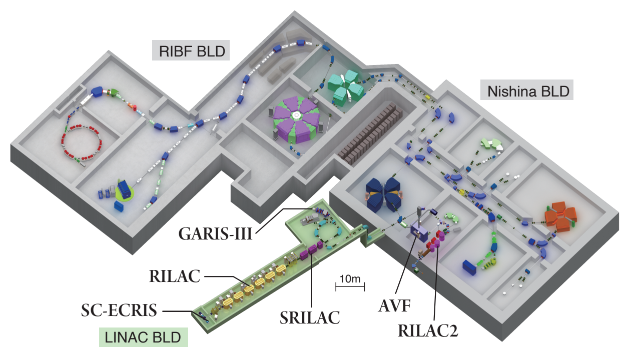

Figure 1: Birds-eye view of the RIBF accelerators.

After the beam commissioning, user beam service started subsequently. After elaborate tuning of the accelerator components, we successfully delivered a ^{51}V beam with an energy ranging from 4.2 to 6.3 MeV/u, thus, was accelerated and delivered proving the required energy and intensity.

For the synthesis of new elements, we expect a long bombarding time in the order of years owing to a small production cross section. Therefore, the reliability of the accelerator hardware is crucial for the success of this long-term project. As lessons learned by the long-term operation the degradation of the SC cavities might pose a significant problem for continuous long-term operations [4]. We observed a sudden increase of field emission (FE) and heavy multipacting (MP). Moreover, the maximum acceleration voltage decreases gradually year by year. In the following sections, we report our experiences collected from the SRILAC over a four-year operation period and provide insights on improving the degradation of the SC cavities.

SRILAC OVERVIEW

The RIKEN superconducting heavy-ion linac (SRILAC) comprises three cryomodules (CMs), CM1, CM2, and CM3,

* nsakamot@ribf.riken.jp

ISBN: 978-3-95450-234-9 ISSN: 2673-5504 doi:10.18429/JACoW-SRF2023-WEPWB085

along with a medium-energy beam transport line (MEBT). The schematic of CM1 and CM2 is shown in Fig. 2. As depicted in the figure, CM1 and CM2 contain four SC-QWRs each (SC01–SC04 and SC05–SC08, respectively). The design of CM3 is identical to that of CM1 and CM2, but two SC-QWRs only (SC09 and SC10). Instead of the traditional top-loading type, bottom-up CMs are used.

The 4 K cold mass consists of a cavity, a helium vessel, a Mu-metal local magnetic shield positioned inside the helium vessel, a fundamental power coupler (FPC), and a dynamic frequency tuner. The cold mass is supported by pillars composed of G10, which is a high-pressure fiberglass lamination, extending from the bottom-base plate, and housed in a vacuum chamber made of steel.

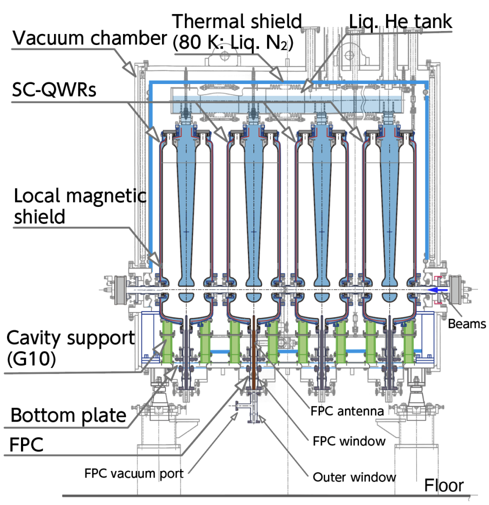

Figure 2: Schematic of the CM1 and CM2.

The specifications of the SC-QWR are listed in Table 1. After the installation of the CMs in the linac building, the

Table 1: SRILAC Design Parameters

Parameters	
Frequency (MHz)	73.0 (CW)
Maximum operation gap voltage (MV)	2.4
Synchronous phase (°)	–25
β_{opt}	0.078
R_{sh}/Q_0 (Ω)	579
G	22.4
E_{acc} (MV/m)	6.8
E_{peak}/E_{acc}	6.2
B_{peak}/E_{acc} (mT/(MV/m))	9.6
Operating temperature (K)	4.5
Target Q_0	1×10^9
Q_{ext}	$1 - 4.5 \times 10^6$
Amplifier output (kW)	7.5

X-ray levels of each SC-QWR were measured during the first high-power RF test, whose results are shown in Fig. 3. However, SC05 was unavailable at that time owing to an issue with the coupler vacuum window occurred during the first cool down to 4 K. The measurements were conducted before opening the gate valves located at the entrance and exit of the CMs. Most of the SC-QWRs exhibited onset gap voltages of approximately 1 MV or higher, followed by the onset of FE. To maintain the initial performance of the SC-QWRs, the SRILAC is equipped with a set of differential pumping systems [5]. These connect the ultra-high-vacuum section, in which no destructive beam monitors (such as FCs) and wire scanners are installed [6], to the RILAC in which the vacuum pressure is about 1e-5 Pa. The CMs are connected with the MEBT, in which the vacuum pressure is about 1e-8 Pa.

Beam tuning was performed carefully to minimize the beam losses in the SRILAC section by measuring the beam transmission efficiency using a set of FCs. Nevertheless, more than half of the ten SC-QWRs experienced an increase in the X-ray levels, thus, necessitating acceleration voltage adjustments for continuous operation.

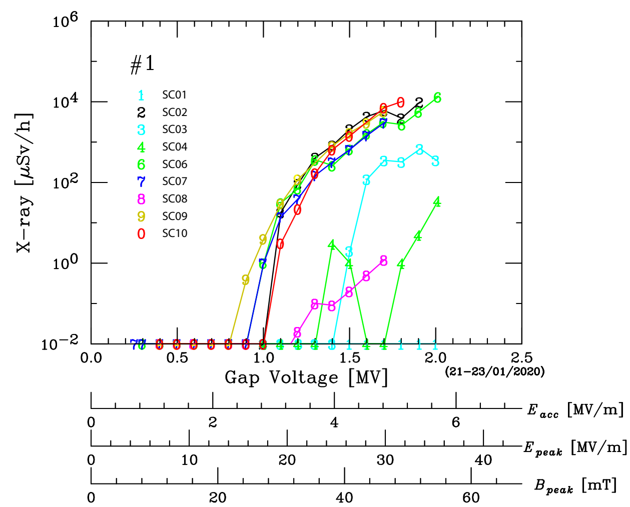

Figure 3: The X-ray levels measured in the first power test at January 2020. The symbols indicate the number of the SC-QWRs.

PERFORMANCE DEGRADATION OF SC-QWRS

The operational history since the first beam-acceleration test, which was performed at the end of January 2020, is shown in Fig. 4. In the figure, blue and orange blocks indicate the duration of the CMs to 4 K and beam operation, respectively. At this stage, the user beam service was operating continuously and we were planning to keep the cooldown for ten months during the current year.

However, we experienced two unexpected interruptions due to unforeseen circumstances. The first interruption was caused by a vacuum issue in CM2. In October 2020, the vacuum level of CM2 suddenly deteriorated owing to a malfunction of the SC06 coupler window. The beam supply was then stopped and, to mitigate the vacuum leak we performed vacuum pumping outside the SC06 coupler. Although the

ISBN: 978-3-95450-234-9 ISSN: 2673-5504 doi:10.18429/JACoW-SRF2023-WEPWB085

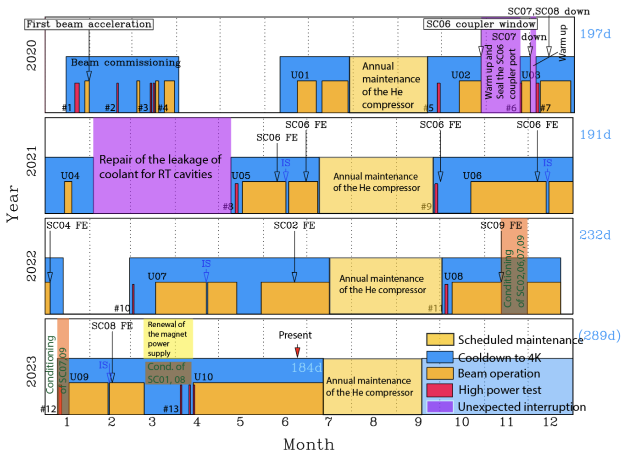

Figure 4: Overview of an operation history of the SRILAC.

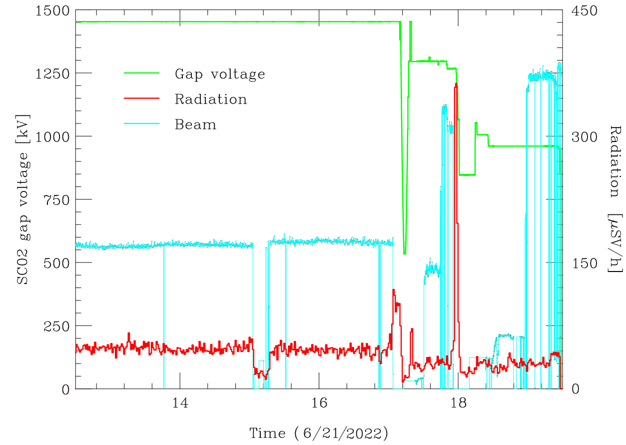

Figure 5: Observation of a sudden increase of X-ray level with SC02.

beam supply was restarted excluding SC06, we encountered serious trouble with SC07 and SC08. In fact, the gap voltages of these cavities often dropped to very low-levels, resulting in MP and in the inability to maintain the acceleration voltages. We attempted to recover the cavity performance by increasing the temperature, however, this was failed. The second interruption caused by a malfunction in the RILAC cavities. During this repair, which required four months, outer vacuum windows were adopted for all the coupler ports of the ten SC-QWRs to protect the coupler windows. In May 2021, their operation was successfully restored [2].

As previously reported [7], the SC-QWRs experienced continuous degradation after the issue with the coupler window of SC06. A gradual increase of the X-ray levels was observed during high-power tests performed routinely after cool-down from room temperature; however, this was not so serious to continue the operation. We repeatedly encountered sudden increases in the X-ray levels, which were continuously measured for each CM during beam service. Consequently, it was necessary to reduce the acceleration voltage of the degraded cavity.

A relevant phenomenon occurred on June 21, 2022, is presented in Fig. 5. The gap voltage and the X-ray levels are plotted in green and red lines, respectively. At 17:01, the X-ray level started to gradually increase during beam supply and reached approximately 120 μSv/h. As shown in the figure, even when the beam supply was stopped, the X-ray level did not decrease. The X-ray level was finally decreased by lowering the gap voltage of the SC02 from 1453 to 535 kV. Initially, reducing the gap voltage to 1296 kV was sufficient. However, at 17:57 the X-ray level suddenly increased again to 350 μSv/h. Therefore, the gap voltage was further decreased to 900 kV, and the X-ray level stabilized at a low level.

The occurrences of similar events are summarized in Table 2. In October 2022, the onset gap voltages of the SC-QWRs became much lower than those of the initial measurement, as shown by the data plotted in Fig. 6. In November 2022, SC09 experienced a significant increase in the X-ray levels, and the available gap voltage became considerably lower than 1 MV. Therefore, we decided to attempt a performance recovery.

Table 2: Events Related to SC-QWRs

Date	Events
10/27/2020	SC06 Vacuum leak
12/1/2020	SC07 down
12/7/2020	SC08 FE increase
12/13/2020	SC07, SC08 down
5/10/2021	10 QWRs operation
6/9/2021	SC06 FE increase
6/29/2021	SC08 FE increase
9/30/2021	SC06 FE increase
12/6/2021	SC06 FE increase
1/3/2022	SC04 FE increase
6/21/2022	SC02 FE increase
11/14/2022	SC09 FE increase
2/15/2023	SC08 FE increase

PROCESSING OF THE DEGRADED SC-QWRS

While several conditioning methods have been employed to address the issues with for SC cavities, a fully established technique has yet to be determined. Therefore, we implemented a conditioning method using high-voltage pulsed RF power, which is relatively simple and imposes a low load on the SC cavities. At KEK (High Energy Accelerator Research Organization), this method was applied to the compact energy recovery linac (cERL) injector cryomodule, and successfully recovered the cavity performance [8].

Because the pulse mode is unavailable with the SRILAC low-level RF (LLRF) system, conditioning had to be implemented using external signal generators. However, a coupler window protection interlock was necessary. The RF power was shut out by a signal from an electron pickup electrode installed in the vicinity of the coupler window. The setup

ISBN: 978-3-95450-234-9 ISSN: 2673-5504 doi:10.18429/JACoW-SRF2023-WEPWB085

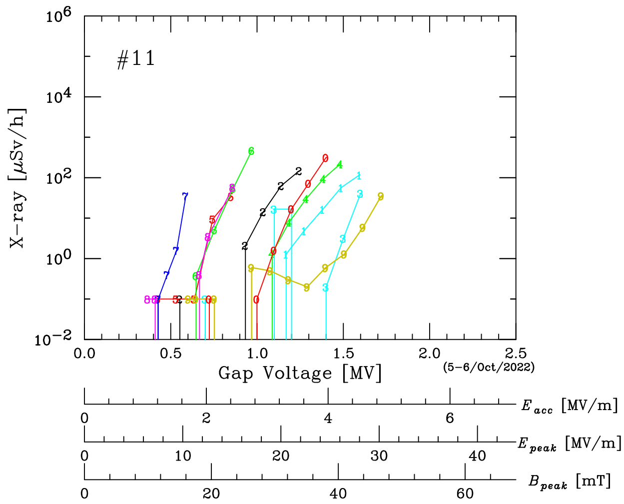

Figure 6: X-ray levels measured in October 2022.

of the conditioning is shown in Fig. 7. Input pulses were

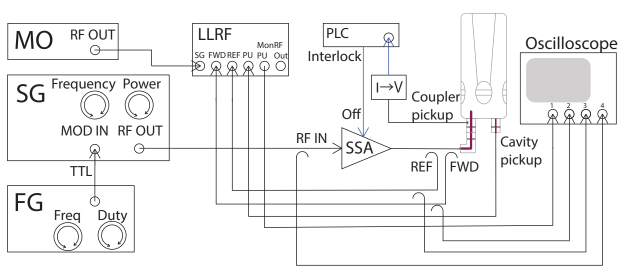

Figure 7: Block diagram for the pulsed RF power conditioning.

produced using the amplitude modulation mode of the signal generator. The amplitude modulation set to 0.5 Hz and a 1% duty RF pulse with a width of 20 ms was adopted. The 20 ms pulse width was sufficient to raise the cavity voltage to up 90% with a detuning of 50 Hz, as shown in Fig. 8. The conditioning was performed by gradually increasing

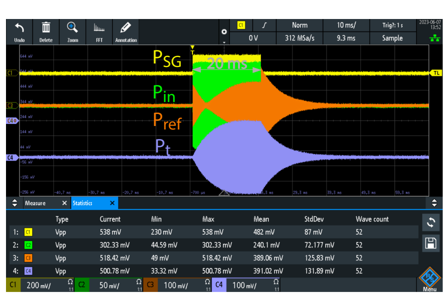

Figure 8: RF signals observed during the pulsed RF power conditioning. P_{SG}, P_{in}, P_{ref}, and P_t, are the input pulse from SG, the forward signal from the directional coupler, the reflected signal, and the signal from the cavity pickup, respectively.

the input RF power. The X-ray levels were compared as a function of the gap voltage before and after conditioning.

The X-ray level recorded during the first conditioning of SC07 is presented as an example in Fig. 9. After the X-ray

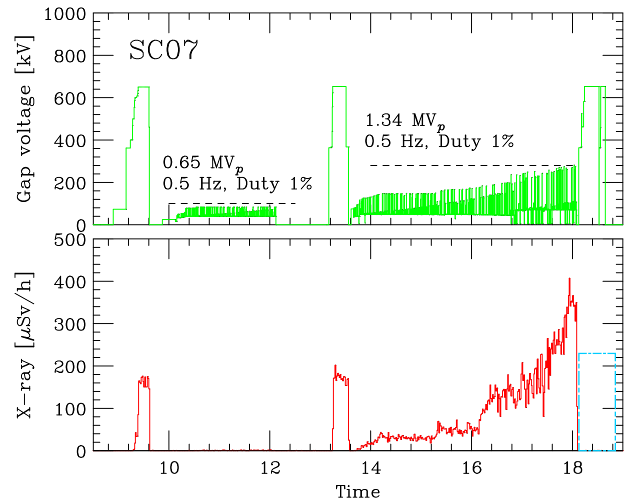

Figure 9: X-ray observed during conditioning.

measurement of 170 μSv/h, the pulsed signal was increased to 0.65 MV and kept constant for 2 h. During this time the observed X-ray level was approximately 1 μSv/h, and no significant change in its value was observed. Subsequently, the pulsed voltage was further increased step wise to 1.34 MV. At a gap voltage of 0.65 MV, the X-ray emission almost vanished. Therefore, our approach has successfully improved the cavity performance, as confirmed by all the following trials listed in Table 3.

Table 3: History of the pulsed RF power conditioning. Here V_p^{max} is a maximum pulsed voltage of the SC-QWRs.

Date	Cavity	Duration(h:mm)	V_p^{max} [MV]
11/22/2022	SC07	7:37	1.34
11/24/2022	SC06	4:05	1.52
11/28/2022	SC09	1:14	1.57
11/29/2022	SC02	0:37	1.98
1/12/2023	SC07	0:54	1.55
1/13/2023	SC09	1:44	1.99
3/29/2023	SC08	2:35	1.80
4/13/2023	SC01	0:40	2.23
6/7/2023	SC09	1:13	2.54

The SC09 cavity was repeatedly conditioned. Conditioning was performed three times by gradually raising the maximum pulsed voltage (V_p^{max}). The onset voltage became increasingly high (see Fig. 10) reaching 1.4 MV higher than that of the initial measurement presented in Fig. 3.

During the conditioning of SC09 in June 2023, some observed phenomena indicated a relationship between FE and MP. As confirmed by previous studies MP occurs around the acceleration gap of the cavity [9]. In Fig. 11, the vacuum pressure of the adjacent MEBT is plotted along with the gap voltage and X-ray levels. Note that the plotted gap voltages

ISBN: 978-3-95450-234-9 ISSN: 2673-5504 doi:10.18429/JACoW-SRF2023-WEPWB085

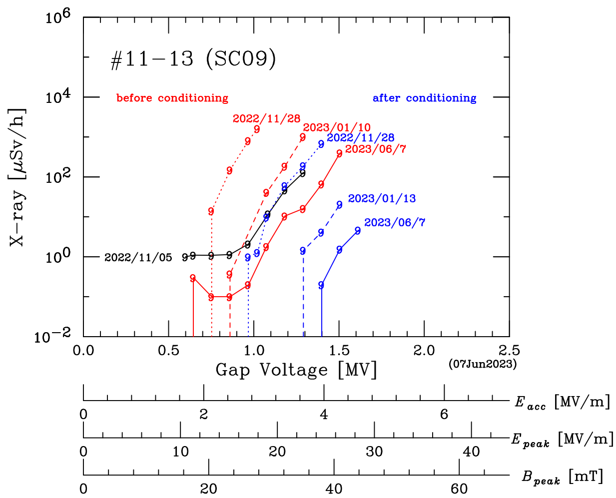

Figure 10: X-ray levels before and after conditioning.

recorded during the conditioning are not scaled because the LLRF system cannot detect the peak power of the pulsed RF signal from the cavity pickup.

The X-ray level, which was initially higher than 300 μSv/h, was successfully reduced to less than 10 μSv/h at a gap voltage of 1.5 MV. Before conditioning, the gap voltage was suddenly dropped, and a low-lying MP was induced. This phenomenon was thought to occur around the acceleration gap because the vacuum pressure of the adjacent MEBT deteriorates owing to the outgassing generated as emitted electrons hit the wall of the beam pipe. Similar phenomena were observed during the conditioning process. Occasionally, a sudden loss of the pickup signal was observed (see Fig. 12), accomplished by variation in the vacuum pressure. After completing the conditioning, MP occurred scarcely.

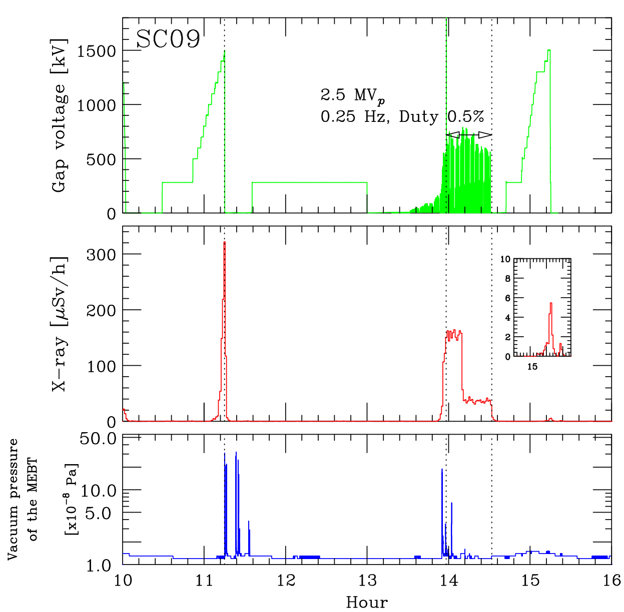

Figure 11: Gap voltage, X-ray level, and the vacuum pressure of the MEBT observed during the conditioning of SC09.

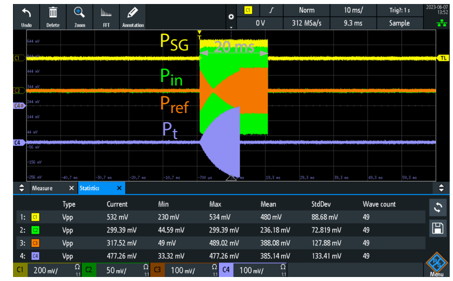

Figure 12: RF signals observed during pulsed rf power conditioning.

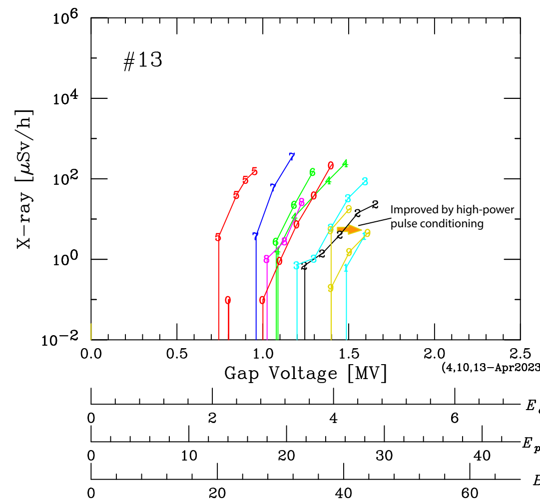

Figure 13: X-ray levels measured in April 2023.

In conclusion, with our SC-QWRs, MP and FE may occur around the acceleration gaps. This explains the effectiveness of pulsed high-power RF conditioning in mitigating MP and FE in our SC-QWRs. The surface cleanliness may be deteriorated by the gas flowing from the MEBT or by some particulates transported by the accelerated beams from the room-temperature-section of the RILAC, in which the vacuum pressure is of approximately 1e-5 Pa. Based on the results of the SC09 conditioning, it was observed that a higher peak power led to a higher onset gap voltage. Although the degradation of SC06 is primarily caused by vacuum leaks from coupler windows, the conditioning appears to be effective. Further investigations will be conducted after replacing the damaged FPCs [10] to gain more insight on these phenomena. Moreover, in future research we will continue to assess the proposed conditioning based on high-power pulsed RFs.

SUMMARY AND FUTURE PLAN

The SRILAC has been in operation for the past four years. However, the degree of performance degradation has become a significant issue, jeopardizing the continuity of operations. Therefore, high-power pulsed RF conditioning was tested to restore the performance. During the period considered in this study, the proposed method successfully limited the

X-ray levels (see Fig. 13). Currently, minimal conditioning is being performed to sustain beam operation. In the near future, we plan to conduct plasma processing test using a prototype cavity.

ACKNOWLEDGEMENT

The authors are grateful to Prof. H. Sakai from KEK for sharing his valuable experience on the pulsed power conditioning of cERL. They also thank Prof. K. Saito for joining our discussion on how to mitigate the degraded cavities. We sincerely thank all the operating staff of the SHI Accelerator Service Ltd. for their effort to ensure the continuous operation of the SRILAC.

REFERENCES

[1] H. Sakai *et al.*, "Facility Upgrade for Superheavy-Element Research at RIKEN", *Eur. Phys. J. A*, vol. 58. pp.238, 2022. doi:10.1140/epja/s10050-022-00888-3

[2] K. Yamada *et al.*, "Successful Beam Commissioning of Heavy-Ion Superconducting Linac at RIKEN", in *Proc. SRF'21*, East Lansing, MI, USA, Jun.-Jul. 2021, pp. 167. doi:10.18429/JACoW-SRF2021-MOOFAV01

[3] H. Okuno *et al.*, "Progress of RIBF Accelerators" *Prog. Theor. Exp. Phys.*, pp. 03C002, 2012. doi:10.1093/ptep/pts046

[4] K. Yamada *et al.*, "Operational Experience for RIKEN Superconducting Linear Accelerator" presented at the SRF'23, Grand Rapids, MI, USA, Jun. 2023, paper MOIXA04, this conference.

[5] H. Imao *et al.*, "Non-Evaporative Getter-Based Differential Pumping System for SRILAC at RIBF", in *Proc. SRF'19*, Dresden, Germany, Jun.-Jul. 2019, pp. 419–423. doi:10.18429/JACoW-SRF2019-TUP013

[6] T. Nishi *et al.*, "Development of Non-Destructive Beam Envelope Measurements in SRILAC with Low Beta Heavy Ion Beams Using BPMs" presented at the SRF'23, Grand Rapids, MI, USA, Jun. 2023, paper MOPMB086, this conference.

[7] N. Sakamoto *et al.*, "Operation Experience of the Superconducting Linac at RIKEN RIBF", in *Proc. SRF'21*, East Lansing, MI, USA, Jun.-Jul. 2021, pp. 315. doi:10.18429/JACoW-SRF2021-MOPFAV005

[8] E. Kako *et al.*, "Degradation and Recovery of Cavity Performances in Compact-ERL Injector Cryomodule", in *Proc. SRF'17*, Lanzhou, China, Jul. 2017, pp. 289–293. doi:10.18429/JACoW-SRF2017-MOPB097

[9] N. Sakamoto *et al.*, "Construction and Performance Tests of Prototype Quarter-wave Resonator and Its Cryomodule at RIKEN", in *Proc. SRF'17*, Lanzhou, China, Jul. 2017, pp. 681–685. doi:10.18429/JACoW-SRF2017-WEYA02

[10] K. Ozeki *et al.*, "Present Status of Riken Power Couplers for SRILAC" presented at the SRF'23, Grand Rapids, MI, USA, Jun. 2023, paper WEPWB101, this conference.